

EXTRACTION AND CHARACTERIZATION OF LIGNIN FROM MOROCCAN THUYA. ITS APPLICATION AS ADSORBENT OF METHYLENE BLUE FROM AQUEOUS SOLUTION

MOHAMMED SABER,* LAHCEN EL HAMDAOUI,*
MOHAMMED EL MOUSSAOUITI* and MOHAMED TABYAOUI*

*Laboratory of Materials, Nanotechnology and Environment, Department of Chemistry,
Faculty of Sciences, Mohammed V University in Rabat, Rabat, Morocco
✉ Corresponding author: L. El Hamdaoui, la.elhamdaoui@gmail.com

Received September 24, 2021

The present investigation includes the extraction of lignin from waste sawdust of the wood industry (*Tetraclinis articulata*) using sulfuric acid treatment, its characterization and further use for the removal of methylene blue (MB) cationic dye from aqueous media. The extracted lignin was characterized by FT-IR and XRD, its thermal properties were studied using TGA and DSC analyses, and its surface morphology was observed by SEM and EDX. The FT-IR spectra showed homogeneity in the chemical structure of the lignin sample. In the adsorption study, the effects of temperature, contact time, and adsorption concentration of MB were determined. The kinetic study showed that the second-order model gives a better description of the kinetics of the adsorption reaction than the first-order model. The analysis of adsorption isotherms using different classical models showed that adsorption may be governed by the Langmuir isotherm. The thermodynamic parameters were determined from the values of the maximum adsorption capacity and equilibrium constants.

Keywords: *Tetraclinis articulata*, lignin, thuya, adsorption, methylene blue

INTRODUCTION

Moroccan Thuya wood industry is dropping approximately tonnes of wood waste annually in the form sawdust. Considering global ecological and economic challenges, this research work envisions the transition of this waste to renewable resources. Several studies have shown the pharmacological properties of extracts from Thuya sawdust, such as antimicrobial,¹ antifungal,² anti-inflammatory,³ and antioxidant.⁴ In this work, we are looking for new uses for valorizing these wood rejects.

Lignin is a complex amorphous polymer composed of phenylpropanoid units, consisting primarily of coniferyl, sinapyl, and *p*-coumaryl alcohols.^{5,6} It is the second most abundant lignocellulosic natural polymer after cellulose and it is mainly found in the cell wall of plant and woody species.⁷ It is regarded as the main source of renewable aromatic structures on earth and is expected to play a role in sustainable production of fuel, functional polymers, aromatic chemicals, phenols, vanillin, ferulic acid, *etc.*⁸ Emerging

trends focus on incorporating lignin in promising future applications, such as controlled drug release, saccharification of lignocelluloses, bioplastics, nanocomposites, nanoparticles, as adsorbents in solution, dispersants, protective UV-absorbents, in electro-chemical applications and carbon fibers.⁷ The utilization of lignin as potential adsorbent has increased in recent years, but it is still in the process of development.⁹ Its bio-based nature and renewability have led to greater focus on its applications in chemical, material and structural industries.

Extensive use of organic products results in their release into effluents, which are then discharged into the environment. Some of them are toxic and interconvertible in the environment; important pollutants thus reach source and treated water, and become a severe public health problem. Moreover, the majority of dyes from different industries may generate toxic substances that present a significant source of environmental contamination when discharged into the

environment without any specific treatment.¹⁰ Therefore, the removal of these contaminants does not depend only on biodegradation.¹¹ Recently, several authors have studied the removal of organic dyes, such as methylene blue (MB), and showed that it has a very good adsorption affinity and high adsorption on solid supports.^{12,13} In this context, several methods have been used: coagulation-flocculation, precipitation, membrane filtration, and electrocoagulation.^{14,15} The adsorption technique has been proven as an efficient, reliable, and low-cost process for the removal of pollutants, namely when the adsorbent is abundant and inexpensive, such as wood wastes and biomaterials.¹⁶ To our knowledge, there are no data reporting the investigation of the isolation and the characterization of lignin from Moroccan *Tetraclinis articulata*.

In this study, the delignification process was performed to isolate Klason lignin from the waste wood of *Tetraclinis articulata*. Klason lignin is the residue obtained after total acid hydrolysis of the carbohydrate portion of wood. Then, the obtained lignin was carefully characterized by several techniques, such as spectroscopic (FT-IR, XRD and SEM-EDX) and thermal analysis (TGA, DTG and DSC). Then, its adsorption capacity was investigated towards a commonly used dye, *i.e.* 3,7-bis (Dimethylamino)-phenothiazin-5-ium chloride (methylene blue, MB), by varying the experimental conditions (residence time, concentration and temperature). The kinetic and thermodynamic parameters of the reaction were established.

EXPERIMENTAL

Materials and reagents

Thuya (*Tetraclinis articulata*) sawdust, as a natural biomass resource, was collected in March 2019 from a local lumber mill in Khemisset, a province of Morocco. Methylene blue (C₁₆H₁₈N₃SCI) and all the chemicals used for the extraction of lignin, such as toluene (C₇H₈), ethanol (C₂H₅OH), and sulfuric acid (H₂SO₄), were purchased from Sigma Aldrich and used without further purification. Distilled water was prepared in the laboratory.

Extraction of lignin

Lignin was isolated from Thuya sawdust by the Klason process. The sawdust was reduced to powder using a micro-grinder, then, 15 g of this powder was treated in a Soxhlet apparatus, using a toluene-ethanol mixture (2:1, v/v). The residue was hydrolyzed with Broxning for 2 hours at room temperature. Then, more water was added to dilute the solution to a 5%

concentration of sulfuric acid. The obtained mixture was boiled for 4 hours, using a flask reactor with a reflux condenser. After that, the insoluble residue was transferred to the filter and washed with distilled water. The obtained lignin was dried at room temperature.¹⁷

The yield of the lignin from the wood sawdust (%) was calculated using the following formula:

$$\text{Yield \%} = \frac{\text{Lignin (g)}}{\text{WoodMaterial (g)}} \times 100 \quad (1)$$

Characterization of extracted lignin

Infrared spectroscopy analysis (IR)

The FT-IR spectrum of the lignin sample was recorded by direct transmittance using a Spectrum FT/IR-4600 (FTIR-ATR: JASCO). The spectrum was recorded in the wavenumber range of 4000-500 cm⁻¹; the number of scans was 20, at a resolution of 4 cm⁻¹. In the Attenuated Total Reflection (ATR) unit, a sufficient amount of sample was placed, without prior preparation. The characteristic bands of lignin were assigned according to the literature.

X-ray diffraction analysis (XRD)

The X-ray diffraction study was performed with a powder X-ray diffractometer (LABXXRD-6100 SHIMADZU), using Cu-K α_1 wavelength of $\lambda = 1.5406$ Å. The scanning angle (2 θ) ranged from 5 to 70° with a step of 0.02°.

Thermogravimetric analysis

The thermogravimetric analyses (TGA) of extracted lignin were performed on a simultaneous thermal analyzer of the LabsysTMEvo (1F) type, of SETARAM brand. The tests were carried out from ambient temperature to 800 °C, with a temperature rise rate of 20 °C/min and an air flow rate of 30 cm³/min. The initial mass of the sample was about 8 mg. Three replicates were used for thermogravimetric analyses.

Differential scanning calorimetry

The thermal behavior of extracted lignin was studied using differential scanning calorimetry (DSC) measurements with a SETARAM DSC 12 type apparatus. The tests were carried out from ambient temperature to 700 °C, under argon with a flow rate of 10 cm³ and a temperature rise rate of 10 °C.min⁻¹. The initial mass of the sample was about 7.7 mg.

Morphological analysis (SEM)

SEM analyses were performed with a Thermo Scientific Quattro S microscope to observe the morphology of extracted lignin. Before imaging, the sample was air dried and coated with a carbon layer to increase conductivity. The microscope was attached to an energy dispersive X-ray analysis (EDX) unit. The image of the sample was examined using an accelerating voltage of 20 kV and different magnifications (x100, x1000 and x2000).

Adsorption study

Adsorption isotherms of methylene blue (MB) were established from a set of aqueous solutions with concentrations varying in the range from 4.10^{-6} to 6.10^{-5} mol.L⁻¹ (i.e. 1.28 mg.L⁻¹ to 19.19 mg.L⁻¹). After adsorption, the concentrations of residual MB were determined by a UV-visible spectrophotometer according to Beer-Lambert's law.

Equilibrium time

The biosorption experiment of MB was conducted by adding 0.05 g of lignin to 20 mL of aqueous solution of 6.10^{-5} mol.L⁻¹ (19.19 mg.L⁻¹) MB dye. The mixture was maintained under agitation at room temperature. The residual concentration of MB was determined for different contact times (from 0 to 180 min), so that the equilibrium time could be evaluated. The following relation was used to calculate the quantity of dye fixed at time t:¹⁸

$$Q_t = \frac{(C_0 - C_t) \times V}{m} \quad (2)$$

where Q_t : the amount of dye adsorbed (mg.g⁻¹) at time t; C_0 : the initial concentration of MB dye (mg.L⁻¹); C_t : the residual concentration at time t (mg.L⁻¹); m : the mass of adsorbent media (g) and V : the volume of solution (L).

Adsorption isotherms

To establish the adsorption isotherms, aqueous solutions of MB were prepared in a concentration range from 4.10^{-6} to 6.10^{-5} mol.L⁻¹. Once the equilibrium was reached, the quantity of adsorbed dye, as well as the residual concentration of dye in the solution, was evaluated. This set of values gives one point of the isotherm.

Thermodynamic parameters

The influence of temperature on the adsorption process of MB onto the lignin material was studied.

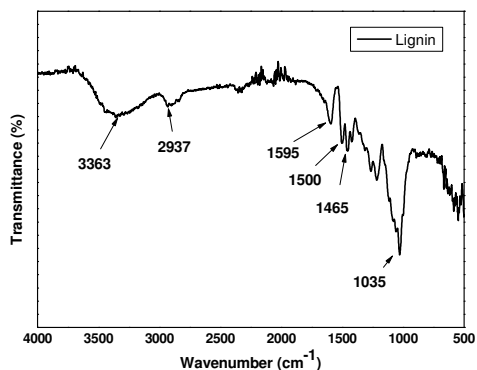


Figure 1: FT-IR spectrum of lignin extracted from Thuya biomass

X-ray diffraction analysis (XRD)

X-ray powder diffraction analysis (XRD) was performed to study the lignin morphology in more

detail. For this series of experiments, the maximum quantity adsorbed by 0.05 g of substrate, in contact with an aqueous solution of MB at 6.10^{-5} mol.L⁻¹ (19.19 mg.L⁻¹), was determined in a temperature range from 25 to 40 °C.

RESULTS AND DISCUSSION

Extraction of lignin from *Tetraclinis articulata*

The sulfuric acid treatment of *Tetraclinis articulata* was chosen to extract lignin, since most of the biomass and, in particular, polysaccharides are hydrolyzed under acidic conditions.¹⁹ Therefore, after the treatment with sulfuric acid, only lignin, char and minerals were expected to remain as solids.²⁰ The obtained yield of the lignin extracted in this study was 36%. This value is in perfect consistency with the literature, which reports that Thuya wood has a chemical composition that is very similar to softwood, but with a higher lignin content (35 to 40%). The lignin content for common softwoods is between 25 and 30%.²¹ Indeed, B. Leopold cited 31.8% as Klason lignin extracted from *Tetraclinis articulata* (Wahl) Mast.²² In another study, Creighton *et al.* reported 29.5% as Klason lignin extracted from *Tetraclinis articulata*.²³

Characterizations of extracted lignin

Infrared spectroscopy analysis (IR)

The FT-IR spectrum analysis of extracted lignin is shown in Figure 1. The FT-IR spectrum reflects the chemical structure of lignin. The spectrum contains characteristic absorption bands, the corresponding assignments and bands for lignin are presented in Table 1.

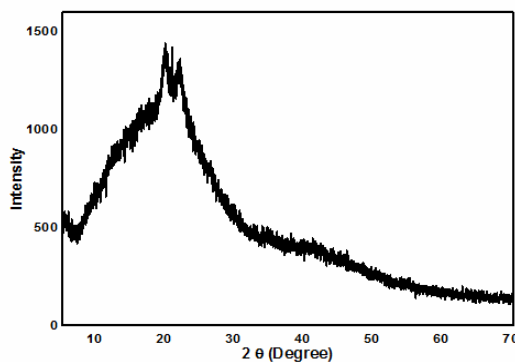


Figure 2: X-ray diffraction pattern of lignin extracted from Thuya biomass

detail. The XRD diffractogram of lignin showed a broad diffraction of amorphous halo, with a maximum at about $2\theta = 20^\circ$ (Fig. 2), which

confirms its natural amorphous character. However, previous research has demonstrated that differences regarding the original source of the lignin, the chemical structure and the extraction method used may explain the variation observed

for the maximum peak of lignin. For example, Goudarzi *et al.*²⁸ and Kubo *et al.*,²⁹ found an average peak for hardwood located at $21.2 \pm 0.15^\circ$ and at 22.7° , respectively.

Table 1
Assignments of FT-IR absorption bands (cm^{-1}) of lignin extracted from Thuya biomass

Wavenumber (cm^{-1})	Assignment/functional group
1035	C–O, C=C, and C–C–O stretching
1215	C–C + C–O stretching
1270	Aromatic ring vibration
1327	C–O stretching of syringyl ring
1335	C–H vibration, O–H in-plane bending
1380	C–H bending
1425	C–H in-plane deformation
1440	O–H in-plane bending
1465	C–H deformation
1500	Aromatic ring vibration
1595	Stretching vibrations $\nu(\text{C}=\text{C})$ in aromatic groups ^{24,25}
2840, 2937	C–H stretching ²⁶
3363	O–H stretching ²⁷

Thermal stability

Thermal analysis is an important technique for determining the physical and chemical properties of polymeric materials as a function of temperature. This work describes the application of TGA and DSC to our lignin extracted from Thuya biomass.

Thermogravimetric analysis

Representative TGA and DTG curves obtained for the combustion of lignin are presented in Figure 3 and its main thermal characteristics from the TGA-DTG curves, such as the temperature of

the degradation onset T_0 , corresponding to 3% mass loss, the temperature of maximum mass loss T_{max} and the percentage of carbon residue (CR%) at T_{max} and at 600°C , are given in Table 2.

In general, the TG-DTG curves of lignin combustion reveal an initial mass loss attributed to the loss of adsorbed and structural water of biopolymers, a region of plateau to about 150°C , a declined deviation extended to about 520°C , where the major mass loss takes place, a final degradation corresponding to the total mass loss, almost to 85%, at 600°C .

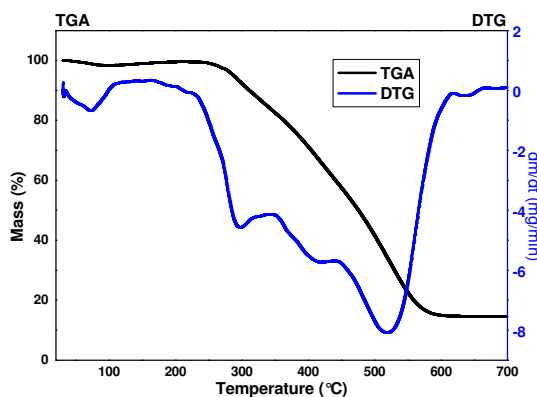


Figure 3: TGA-DTG curves of lignin extracted from Thuya biomass

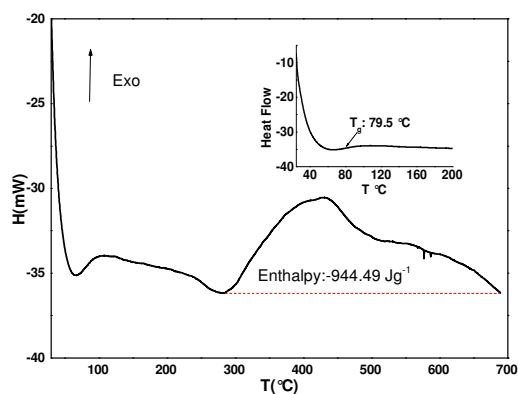


Figure 4: DSC thermogram of lignin extracted from Thuya biomass obtained at $10^\circ\text{C}\cdot\text{min}^{-1}$

Table 2
Thermal characteristics of lignin extracted from Thuya biomass

Sample	T ₀ (°C)	T _{max} (°C)	CR ^a (%) (at T _{max})	CR ^b (%) (at 600 °C)
Extracted lignin	240	517	34	15

T₀: temperature of degradation onset to 3% mass loss; T_{max}: temperature of maximum mass loss; CR^a(%): percentage of carbon residue at T_{max}; CR^b(%): percentage of carbon residue at 600 °C

This degradation behavior is attributed to thermal decomposition of polymeric chains of carbohydrates, with vaporization of volatile compounds. The DTG curve evidences a small peak, which is due to moisture loss, a sharp maximum at 100 °C. This early ignition of biomass is a key factor in the earlier completion of volatile combustion and the consequential improvement in particle burnout.³⁰ In the first stage, decomposition of biomass components (hemicelluloses, cellulose and lignin) takes place and the next stage is the combustion of the complex and thermally stable structure.^{31–34}

Differential scanning calorimetry (DSC) analysis

The thermal stability of the lignin extracted from Thuya biomass was determined in this study through DSC analysis, where the heat of reaction was measured (Fig. 4).

The DSC curve of Klason lignin shows two endothermic peaks, followed by an exothermic peak. The first, below 100 °C, corresponds to dehydration, the second weight loss event, at 285 °C, may be due to the traces of carbohydrates – when the lignin is not pure enough, the mass loss that occurs after dehydration is attributed to the decomposition of carbohydrates.³⁵ The exothermic peak is associated with the decomposition of the lignin. From the DSC experiment (Fig. 4), the estimated enthalpy value associated with the pyrolysis of the lignin is -944.49 Jg^{-1} . Previous research has shown that the measured enthalpy of lignin depends on the biomass resources, and the source of lignin samples was seen to affect the thermal properties.³⁶ The results suggest that more energy is required to break down the bonds in the composition of lignin extracted from Thuya biomass, yielding a more stable and flame retardant biomaterial.

The glass transition temperature (T_g) is one of the most important thermodynamic parameters of biomaterials, it is reliable and convenient to expound the phase behavior of macromolecules. Therefore, based on the literature, the T_g value is

very broad, ranging from ~120 to 190 °C.^{37,38} This wide range may be explained by various molecular parameters, such as rigid phenyl groups, interchain hydrogen-bonding, crosslinking density, and molecular mass.³⁹ The T_g is also dependent on the plant source, extraction conditions, and difference between different lignins in terms of flexibility and stiffness at elevated temperatures, which is important in industrial applications.

The obtained T_g = 79.5 °C value for the lignin extracted in this work, using the Klason method, is lower than other values reported in the literature. Kubo and Kadla, studying commercial kraft lignins from hardwood and softwood obtained T_g values of 93 °C and 119 °C, respectively.²⁹ Tejado *et al.* found T_g values of 100 °C and 144 °C for lignins obtained by organosolv and kraft isolation methods.⁴⁰ Therefore, the actual numerical value could not be regarded as sufficiently reliable.

Morphological analysis

The study of the morphology of lignin extracted from Thuya was carried out by a Thermo Scientific Quattro S scanning electron microscope, equipped with an EDX system. Figure 5 displays the SEM images of the morphological structure of lignin studied at different magnification: x100 (a), x1000 (b), and x2000 (c). It can be noted that the lignin appeared granulated, with grains of compact structure and different sizes creating platelet agglomeration, and some spaces that are apparently occupied by bubbles. Also, we can observe microcavities on the surface of the lignin, which seem to indicate a very porous irregular structure, favorable for its use as adsorbent, ensuring good diffusion of dye molecules.

The EDX analysis of this biomaterial (Fig. 6) shows the presence of major elements, such as carbon (C 53.54%) and oxygen (O 45.77%), and traces of silicon (Si 0.37%) and aluminum (Al 0.32%). The carbon is an essential, main element of the structural constituents of lignin and cellulose. The higher proportion of carbon in

lignin can be correlated with the amount of aromatic carbons from lignin subunits (*p*-hydroxyphenyl, guaiacyl, and syringyl). Also, the

higher carbon content observed for our lignin can be, therefore, explained by its higher purity.

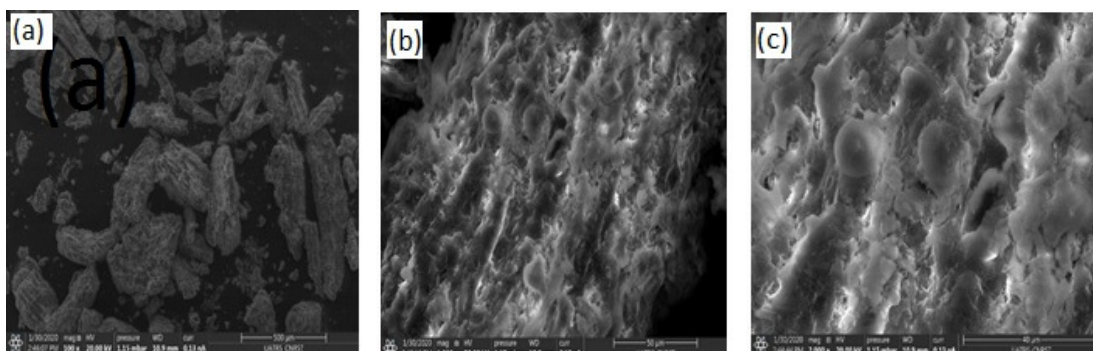


Figure 5: SEM images of lignin processed at different magnification (a) x100, (b) x1000, and (c) x 2000

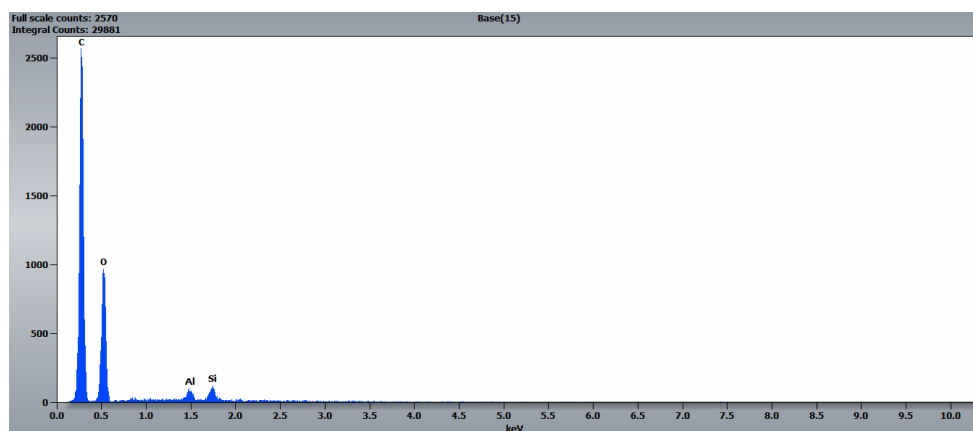


Figure 6: EDX analysis of lignin extracted from Thuya

Methylene blue adsorption

This work presents the evaluation of lignin extracted from Thuya (*Tetraclinis articulata*) used as adsorbent for the removal of methylene blue dye (MB) from aqueous solution. From the calibration plot (Fig. 7), we have verified that the absorbance varies linearly with the adsorbate concentration, which shows that Beer Lambert's law is verified. The calibration curve is established with a correlation coefficient $R^2 = 0.957$.

Kinetics studies

Several mathematical models are given in the literature to describe the adsorption kinetics. All these models bring some information on the adsorption rate and mechanism of the adsorption. These formalisms have been chosen because they are quite simple and thus commonly used when dealing with the adsorption of organic compounds on various adsorbents. Figure 8 shows the

adsorption kinetics of methylene blue onto the lignin material. It can be seen that the adsorption of MB is faster, the adsorption equilibrium is reached in 140 minutes, by establishing a well-formed plateau, also indicating that lignin is a very effective adsorbent acting in a short time, and the adsorption rate is about 3.55 mg/g. This fast rate of adsorption can be due to the number of active sites and the porous irregular structure on the surface of the lignin material, as well as to the interaction of functional groups with the lignin surface.

As may be seen below, lignin appears as a very promising sorbent considering that it is very inexpensive, effective and can be obtained from locally available materials. It exhibits adsorptive characteristics towards toxic organic molecules from aqueous solution. Generally, the efficiency of the adsorption increases with the surface area of the adsorbent, but sometimes, this adsorption involves the interaction between the material

surface and the functional groups of toxic organic molecules, including sharing of electrons between the pollutant and the surface of the adsorbent, resulting in chemical bonds.

In this study, we applied different kinetic models to describe the adsorption kinetic mechanism, namely, the first order,⁴¹ pseudo-second order, and second-order reaction models.^{42,43}

The Lagergren kinetic model of adsorption gives⁴¹ for first order reaction:

$$\log(Q_e - Q_t) = \log Q_e - K_1 \frac{t}{2.3} \quad (3)$$

While carrying $\log(Q_e - Q_t)$ versus t (Fig. 9), a straight line should be obtained, whose slope gives K_1 , the rate constant of adsorption (min^{-1}). From this plot, one can extract the values of K_1 and Q_e parameters and they are given in Table 4.

It is clear from the analysis of $\log(Q_e - Q_t)$ as a function of time that it is not linear, and consequently, the adsorption of methylene blue on lignin cannot be described by the first order model.

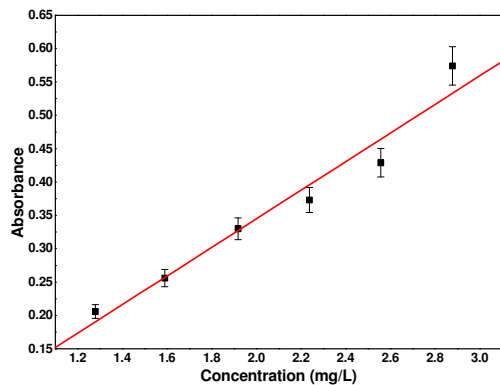


Figure 7: Methylene blue (MB) calibration curve

After this result, we applied the pseudo-second reaction to fit the experimental data obtained from the kinetic experiments. The rate constant K_2 is given by the following relation:^{42,43}

$$\frac{t}{Q_t} = \frac{1}{2K_2Q_e^2} + \frac{t}{Q_e} \quad (4)$$

where Q_e and Q_t designate the absorption capacity (mg/g) at equilibrium and time t , respectively. K_2 represents the constant rate of adsorption (g/mg.min).

The parameters Q_e and K_2 are obtained by representing t/Q_t versus t (Fig. 10). The obtained values for these parameters are gathered in Table 4.

For the second order reaction, the rate constant K_3 results from the following relation:^{42,43}

$$\frac{1}{Q_e - Q_t} = \frac{1}{Q_e} + K_3 \times t \quad (5)$$

where, in all the cases, Q_e : quantity adsorbed at equilibrium (mg.g^{-1}), Q_t : quantity adsorbed at time t (mg.g^{-1}), t : contact time (min). Thus, K_3 is determined from the chart of $1/(Q_e - Q_t)$ versus t .

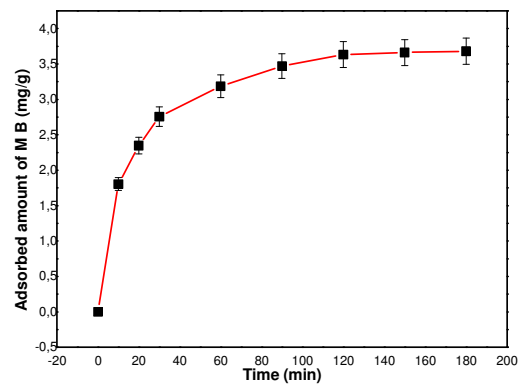


Figure 8: Effect of contact time on methylene blue adsorption

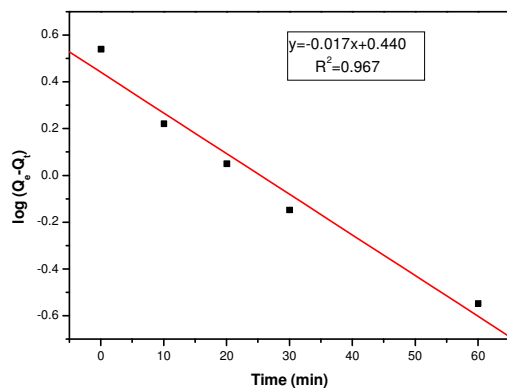


Figure 9: $\log(Q_e - Q_t)$ versus time according to the first-order kinetic model

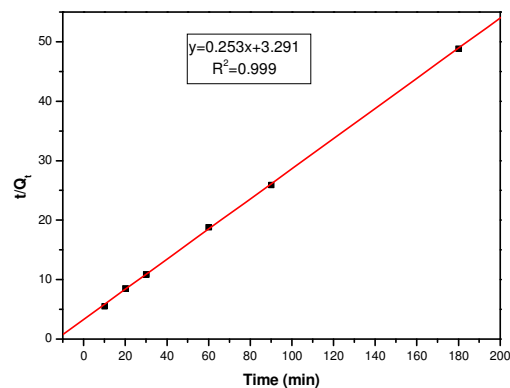


Figure 10: t/Q_t versus time according to the pseudo-second order kinetic model

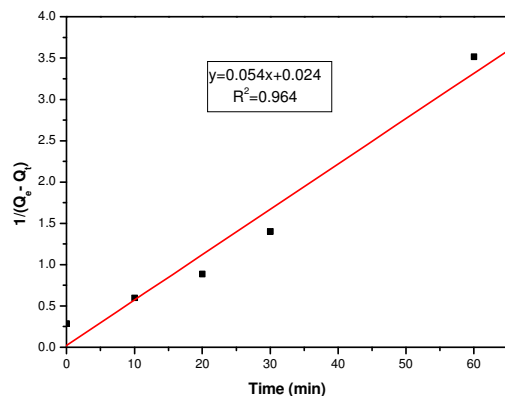

 Figure 11: $1/Q_e - Q_t$ versus time according to the second order model

 Table 4
 Kinetic constants and adsorption capacities calculated for different models studied

Q_e Exp. (mg/g)	First order			Pseudo-second order			Second order		
	K_1	Q_e calc. (mg/g)	R^2	K_2	Q_e calc. (mg/g)	R^2	K_3	Q_e calc.	R^2
3.55	0.0391	1.66	0.967	0.009	3.95	0.999	0.054	47.66	0.964

The linear variation (Fig. 10) of t/Q_t over time suggests that the pseudo-second order model describes well the kinetic behavior of MB adsorption onto the extracted lignin. The experimental data can be fitted with the equation: $t/Q_t = 0.2536t + 3.2915$, with a correlation coefficient $R^2 = 0.9998$. The analysis of the data given in Table 4 showed perfectly that the experimental adsorption capacity Q_e is very close to that obtained by the pseudo-second order reaction. Therefore, according to this latter model, we can state that the adsorption of methylene blue on the lignin involves chemisorption, in addition to physisorption. It is clear from the analysis of $1/Q_e - Q_t$ as a function of time (Fig. 11) that it is not linear, and consequently, the adsorption of

methylene blue on lignin cannot be described by the second order reaction.

Comparison with other adsorbents

The initial concentration of MB, reaction time, and adsorption quantity (Q_e) of MB by extracted lignin have been compared with other adsorbents reported in the literature, which are listed in Table 5. Despite numerous results reported in the literature, the advantage of using Klason lignin extracted from *Tetraclinis articulata* lies in its abundance and ease of extraction. These properties, which cannot be attributed to all adsorbents, are essential for developing low-cost adsorbents and their application at an industrial scale.

 Table 5
 Comparison of initial concentration of MB, reaction time and adsorbed quantity (Q_e) of MB onto lignin extracted in this study with those for other reported adsorbents

Adsorbent	Initial MB concentration (mg/L)	Reaction time (min)	Adsorbed quantity Q_e exp. (mg/g)	Reference
Pure cellulose	19.19	80	0.11	44
Modified cellulose	19.19	80	0.35	44
Thuya lignin	19.19	140	3.55	This study
Algerian date stones	100	60	4.9	45
Acetic acid lignin	50	60	24.6	46
ZnCl ₂ activated carbon	6.0	180	29.968	47
Algerian kaolin	80	120	36.80	48
Tunisian natural lignin	300	240	78	49

It can be considered that the lignin extracted from waste Thuya biomass tested herein is effective in the removal of MB from aqueous solutions and, moreover, it may be used as an alternative to expensive commercial adsorbents

Adsorption isotherms

The adsorption isotherms of MB onto the lignin material were obtained by plotting the amount of dye adsorbed by the substrate (Q_e) as a function of the residual dye concentration in solution at equilibrium (C_e) at 25 °C. The contact time between dye and adsorbent was fixed at 3 hours, assuming that equilibrium is reached and that there is no significant variation in the concentration of the dye (only 90 minutes were necessary with MB solution at 6.10^{-5} mol.L⁻¹ (19.19 mg.L⁻¹) as previously mentioned).

The adsorption isotherms describe the distribution of MB dye between the solution and the lignin adsorbent when the adsorption process reaches an equilibrium state. It is mandatory, as it allows to better understand the mechanisms involved in the adsorption process. There are several applicable isotherm models, but the two most commonly used models are those of Langmuir and Freundlich.^{50,51} The Langmuir model describes the adsorption behavior of homogeneous surfaces. It is based on the following assumptions: strong uniform adsorption sites, no interactions between adsorbed molecules, the adsorption occur through the formation of a monolayer of adsorbate.⁵² The linear form of this isotherm is represented as follows:

$$Q_e = Q_m - \left(\frac{1}{K_L}\right) \times \frac{Q_e}{C_e} \quad (6)$$

where Q_e (mg.g⁻¹) is the amount of dye adsorbed at equilibrium, C_e (mg.L⁻¹) is the equilibrium concentration, K_L (l/g) is the Langmuir constant and Q_m is the monolayer adsorption capacity.

In addition, the essential characteristic of the Langmuir isotherm can be expressed by a dimensionless term called the R_L separation factor (Eq. 7), defined as a unitless quantity, indicating the nature of the adsorption, “favorable” or “unfavorable”. This factor is used to predict whether an adsorption system is “favorable” or “unfavorable”. The adsorption is said to be favored when R_L tends towards zero and it is disadvantaged when R_L tends towards unity.⁵³ It is defined as:

$$R_L = \frac{1}{1 + K_L \cdot C_0} \quad (7)$$

The Freundlich model is based on an empirical equation, which expresses a change in adsorption energy with the amount adsorbed.⁵¹ This distribution is explained by the heterogeneity of adsorption sites and this model admits the existence of interactions between adsorbed molecules.⁵⁴ Equation 8 represents the Freundlich isotherm:

$$Q_e = K_F \times C_e^{1/n} \quad (8)$$

where Q_e is the amount of solute adsorbed per unit weight of adsorbent (mg.g⁻¹), C_e is the equilibrium concentration, K_F is the Freundlich constant and (n) is the heterogeneity factor. The value K_F is related to the adsorption capacity, while the value of ($1/n$) is related to the adsorption intensity. When $n = 1$, the adsorption is linear, meaning that the sites are homogeneous and there is no interaction between the adsorbed species; when $1/n < 1$, adsorption is favorable and the adsorption capacity increases while new adsorption sites appear. When $1/n > 1$, adsorption is not favorable, adsorption bonds become weak and the adsorption capacity decreases.⁵⁵

Let us now to consider the above models. The Langmuir isotherm equation (6) was applied to the adsorption data to quantify the adsorption capacity of the lignin. The Langmuir plot (Fig. 12) of the data displayed a good linear fit and the K_L parameter from the slope and intercept is presented in Table 6. From the table, one can note that the correlation coefficient R^2 ($R^2 = 0.997$) is close to 1. The calculated value of R_L is 0.23, which indicates that the adsorption system is favorable.

In parallel, the adsorption data were also plotted using the Freundlich model under the same experimental conditions (Fig. 13). The calculated values of K_F and ($1/n$) are gathered in Table 6. The value of $1/n = 0.3$ indicates that the adsorption using heterogeneous sites is favorable. Nevertheless, based on the correlation coefficient (R^2) values in the present study, the Langmuir isotherm provides the best fit for the experimental data.

The values of the correlation coefficients confirm the better fit of the experimental data to the isothermal model of Langmuir than to that of Freundlich. These values indicate that the adsorption process of methylene blue dye onto lignin is described favorably by the Langmuir isotherm. Thus, the results obtained show that the Klason lignin extracted from *Tetraclinis articulata* waste sawdust of the wood industry is a

very efficient tool for the elimination of MB dye, and this may be due to its chemical composition

and its very porous structure.

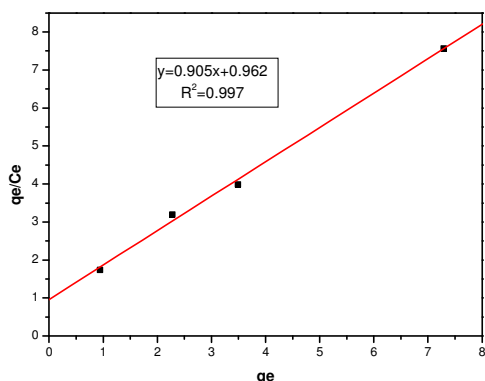


Figure 12: Langmuir plot for MB adsorption on lignin

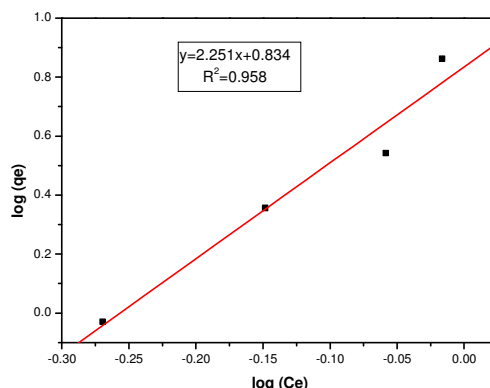


Figure 13: Freundlich plot for MB adsorption on lignin

Table 6
Calculated values of adsorption parameters for Freundlich and Langmuir models

Langmuir adsorption model	Freundlich adsorption model
$R^2 = 0.997$	$R^2 = 0.958$
$K_L (l/mg) = 1.104$	$K_F (l/Kg) = 6.823$
$R_L = 0.239$	$1/n = 0.307$

Thermodynamic parameters

The most important thermodynamic parameters, such as enthalpy of reaction ΔH° , entropy ΔS° , and Gibbs free energies ΔG° , were calculated, as indicated by Albadarin *et al.*,⁵⁶ to understand the adsorption process by quantifying the energy involved in it. The numerical values of ΔH° , ΔS° , and ΔG° for the adsorption of MB onto the extracted lignin are listed in Table 7. The positive value of ΔH° obtained indicated that the adsorption process was endothermic in nature. The ΔS° value obtained reflects the affinity of the adsorbent towards the adsorbate, suggesting the increased randomness at the solid/solution interface during the adsorption process.⁵⁷ The negative value of Gibbs free energy ΔG° indicates that the adsorption process is spontaneous and favored at low temperature; the decrease in the ΔG° values with temperature suggests that the process is feasible at higher temperatures.⁵⁸ The equilibrium constant for MB adsorption onto a substrate is given by the relationship:

$$K_c = \frac{(C_0 - C_e)}{C_e} \tag{9}$$

where C_0 is the initial concentration ($mg.L^{-1}$) and C_e is the equilibrium concentration ($mg.L^{-1}$), K_c is related to the Gibbs energy of reaction, ΔG° , by $\Delta G^\circ = -R.T.Ln(K_c)$ and therefore: $Ln(K_c) = -\Delta H^\circ/RT + \Delta S^\circ/R$, where ΔH° and ΔS° are, respectively, the enthalpy and standard entropy of adsorption, which can be assessed by plotting $Ln(K_c)$ versus $1/T$ (Fig. 14). The results are reported in Table 7.

Adsorption mechanisms

In general, the adsorption mechanism depends on the surface of the adsorbent and the structure of the dye molecule. It is important to understand the adsorption process, which can be complex and involve more than one mechanism.^{59,60} Figure 15 shows the proposed possible mechanism for adsorption of MB dye onto the surface of the lignin extracted from Thuya.

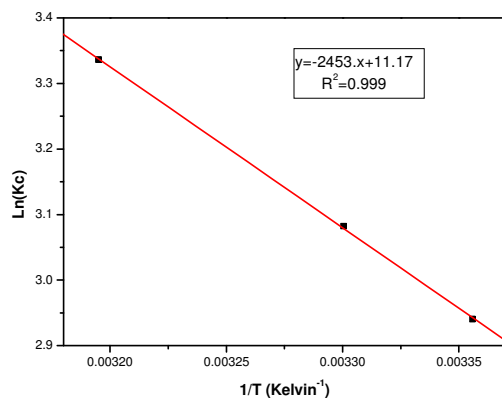
Figure 14: Ln(K_c) versus $1/T$

Table 7
Thermodynamic parameters associated with the adsorption process

ΔH° (kJmol ⁻¹) (25 °C)	ΔS° (JK ⁻¹ mol ⁻¹) (25 °C)	ΔG° (kJmol ⁻¹)
		-7.286601 (25°C)
20.39424	92.86738	-7.765476 (30°C)
		-8.68295 (40°C)

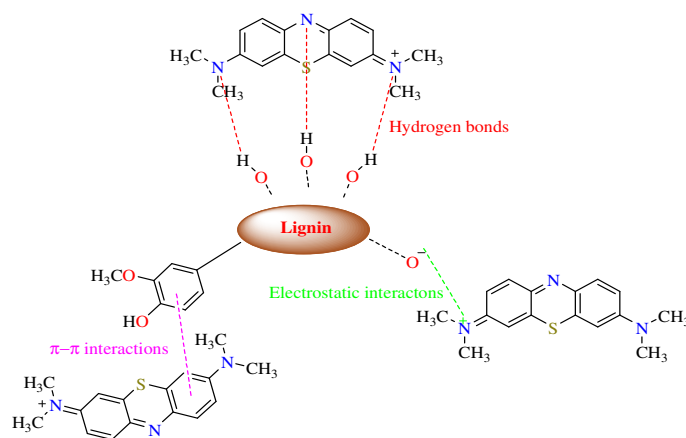


Figure 15: Proposed mechanism of MB adsorption onto lignin

In this study, three interactions can be suggested as having possibly occurred during MB dye adsorption onto the lignin. Firstly, FT-IR analysis showed oxygen functional groups (-OH and -OCH₃) derived from the major structural components of lignin, which may have interacted through van der Waals forces and hydrogen bonds with the MB molecule. Secondly, the reaction between deprotonated groups of lignin (C-O-group) and the cationic species, such as MB, may be accelerated due to the electrostatic force of attraction. Finally, $\pi - \pi$ cyclic interactions may have occurred due to the presence of aromatic systems in the structures of lignin monomers (*p*-coumaryl alcohol, coniferyl alcohol, and sinapyl alcohol) and the structure of the MB dye

molecule. In addition, numerous studies confirm that these three types of interactions can occur in the adsorption of MB dye.⁶¹⁻⁶⁴

CONCLUSION

The present investigation focused on the extraction of lignin from *Tetraclinis articulata* waste sawdust of the wood industry, using sulfuric acid treatment, which was then characterized through FT-IR, XRD, thermogravimetric analysis (TGA), and differential scanning calorimetry (DSC). The surface morphology of the extracted lignin was analyzed by SEM and EDX analyses. FT-IR spectra showed homogeneity in the chemical structure of the lignin sample extracted after the

treatment with sulfuric acid. The sulfuric acid treatment showed good performance in terms of the lignin yield from *Tetraclinis articulata*, with a percentage extraction yield close to 36%. DSC analysis was used to determine the heat of reaction of the lignin sample. Enthalpy measurements were higher for lignin from *Tetraclinis articulata*: -944.49 J/g. TGA analysis was used to study the degradation of the biomaterial. Then, we have tested the adsorption of cationic dye MB onto lignin by varying the experimental conditions (contact time, concentration and temperature). The kinetic and thermodynamic parameters of the reaction have been established. The results showed that the adsorption kinetics of MB on lignin was well described by the pseudo-second order. The adsorption isotherms were described satisfactorily by the Langmuir model. The temperature had a positive effect on the adsorption of MB, suggesting that it is an endothermic process.

The findings of the present study will encourage using low-cost adsorbent materials in the removal of dyes from industrial wastewater. Further work will be carried out to explore the suitability of the lignin adsorbent for the removal of other textile dyes.

REFERENCES

- ¹ A. Talbaoui, L. El Hamdaoui, M. El Moussaouiti, M. Aneb, S. Amzazi *et al.*, *J. Indian Acad. Wood Sci.*, **13**, 114 (2016), <https://doi.org/10.1007/s13196-016-0173-7>
- ² A. Fidah, N. Salhi, T. Janah, M. Rahouti, B. Kabouchi *et al.*, *J. Indian Acad. Wood Sci.*, **13**, 132 (2016), <https://doi.org/10.1007/s13196-016-0174-6>
- ³ A. Djouahri, S. Boualem, L. Boudarene and A. Baaliouamer, *Ind. Crop. Prod.*, **63**, 138 (2015), <https://doi.org/10.1016/j.indcrop.2014.10.018>
- ⁴ M. Saber, H. Hicham, A. Bouyahya, T. Ouchbani and M. Tabyaoui, *Biointerface Res. Appl. Chem.*, **11**, 7912 (2021), <https://doi.org/10.33263/BRIAC111.79127920>
- ⁵ R. Hatfield and W. Vermerris, *Plant Physiol.*, **126**, 1351 (2001), <https://doi.org/10.1104/pp.126.4.1351>
- ⁶ T. Sugimoto, T. Akiyama, Y. Matsumoto and G. Meshitsuka, *Holzforschung*, **56**, 416 (2002), <https://doi.org/10.1515/HF.2002.064>
- ⁷ M. Norgren and H. Edlund, *Curr. Opin. Colloid Interface Sci.*, **19**, 409 (2014), <https://doi.org/10.1016/j.cocis.2014.08.004>
- ⁸ A. Duval and M. Lawoko, *React. Funct. Polym.*, **85**, 78 (2014), <https://doi.org/10.1016/j.reactfunctpolym.2014.09.017>
- ⁹ Suhas, P. J. M. Carrott and M. M. L. Ribeiro Carrott, *Bioresour. Technol.*, **98**, 2301 (2007), <https://doi.org/10.1016/j.biortech.2006.08.008>
- ¹⁰ O. Hamdaoui, F. Saoudi, M. Chiha and E. Naffrechoux, *Chem. Eng. J.*, **143**, 73 (2008), <https://doi.org/10.1016/j.cej.2007.12.018>
- ¹¹ N. Kannan and M. M. Sundaram, *Dyes Pigm.*, **51**, 25 (2001), [https://doi.org/10.1016/S0143-7208\(01\)00056-0](https://doi.org/10.1016/S0143-7208(01)00056-0)
- ¹² S. Shukla, S. A. L. Dwivedi, K. Sharma, D. Bhargava *et al.*, *Int. J. Sci. Innov. Res.*, **2**, 58 (2014)
- ¹³ D. Ghosh and K. G. Bhattacharyya, *Appl. Clay Sci.*, **20**, 295 (2002), [https://doi.org/10.1016/S0169-1317\(01\)00081-3](https://doi.org/10.1016/S0169-1317(01)00081-3)
- ¹⁴ S. Kacha, M. S. Ouali and S. Elmaleh, *Rev. Sci. Eau.*, **10**, 233 (1997)
- ¹⁵ H. S. Shin and J. K. Lee, *Korean J. Chem. Eng.*, **23**, 188 (2006), <https://doi.org/10.1007/BF02705714>
- ¹⁶ A. Bhatnagar and M. Sillanpaa, *Chem. Eng. J.*, **157**, 277 (2010), <https://doi.org/10.1016/j.cej.2010.01.007>
- ¹⁷ B. L. Browning, "Methods of Wood Chemistry", Interscience Publishers, N.Y., 1967
- ¹⁸ Y. S. Ho, *Carbon*, **42**, 2115 (2004), <https://doi.org/10.1016/j.carbon.2004.03.019>
- ¹⁹ L. Fan, M. M. Gharpuray and Y. H. Lee, "Cellulose Hydrolysis", Springer, Berlin, Heidelberg, 1987, pp. 121-148, https://doi.org/10.1007/978-3-642-72575-3_4
- ²⁰ P. T. Patil, U. Armbruster, M. Richter and A. Martin, *Energ. Fuels*, **25**, 4713 (2011), <https://doi.org/10.1021/ef2009875>
- ²¹ A. Haddad, D. Lachenal, A. Marechal, M. Kaid-Harche and G. Janin, *Ann. For. Sci.*, **63** (2006), <https://doi.org/10.1051/forest:2006030>
- ²² B. Leopold, *Acta Chem. Scand.*, **6**, 49 (1952), <https://doi.org/10.3891/acta.chem.scand.06-0049>
- ²³ R. H. J. Creighton, R. D. Gibbs and H. Hibbert, *J. Am. Chem. Soc.*, **66**, 32 (2002), <https://doi.org/10.1021/ja01229a010>
- ²⁴ O. Faix and O. Beinhoff, *J. Wood. Chem. Technol.*, **8**, 505 (1988), <https://doi.org/10.1080/02773818808070698>
- ²⁵ U. Kües, "Wood Production, Wood Technology, and Biotechnological Impacts", 2007, <https://doi.org/10.17875/gup2007-262>
- ²⁶ O. Y. Abdelaziz and C. P. Hulteberg, *Waste Biomass Valor.*, **8**, 859 (2017), <https://doi.org/10.1007/s12649-016-9643-9>
- ²⁷ L. K. Kian, M. Jawaid, H. Ariffin and O. Y. Alothman, *Int. J. Biol. Macromol.*, **103**, 931 (2017), <https://doi.org/10.1016/j.ijbiomac.2017.05.135>
- ²⁸ A. Goudarzi, L. T. Lin and F. K. Ko, *J. Nanotechnol. Eng. Med.*, **5** (2014), <https://doi.org/10.1115/1.4028300>
- ²⁹ S. Kubo and J. F. Kadla, *J. Polym. Environ.*, **13**, 97 (2005), <https://doi.org/10.1007/s10924-005-2941-0>
- ³⁰ T. Abbas, P. Costen, N. H. Kandamby, F. C. Lockwood and J. J. Ou, *Combust. Flam.*, **99**, 617 (1994), [https://doi.org/10.1016/0010-2180\(94\)90055-8](https://doi.org/10.1016/0010-2180(94)90055-8)

- ³¹ S. W. Park, C. H. Jang, K. R. Baek and J. K. Yang, *Energy*, **45**, 676 (2012), <https://doi.org/10.1016/j.energy.2012.07.024>
- ³² H. Yang, R. Yan, H. Chen, C. Zheng, D. H. Lee *et al.*, *Energ. Fuels*, **20**, 388 (2006), <https://doi.org/10.1021/ef0580117>
- ³³ C. Fushimi, K. Araki, Y. Yamaguchi and A. Tsutsumi, *Ind. Eng. Chem. Res.*, **42**, 3929 (2003), <https://doi.org/10.1021/ie0300575>
- ³⁴ H. Yang, R. Yan, H. Chen, D. H. Lee and C. Zheng, *Fuel*, **86**, 1781 (2007), <https://doi.org/10.1016/j.fuel.2006.12.013>
- ³⁵ P. Manara, A. Zabaniotou, C. Vanderghem and A. Richel, *Catal. Today*, **223**, 25 (2014), <https://doi.org/10.1016/j.cattod.2013.10.065>
- ³⁶ D. Watkins, Md. Nuruddin, M. Hosur, A. Tcherbi-Narteh and S. Jeelani, *J. Mater. Res. Technol.*, **4**, 26 (2015), <https://doi.org/10.1016/j.jmrt.2014.10.009>
- ³⁷ J. Sameni, S. Kristin, D. dos S. Rosa, A. Leao and M. Sain, *BioResources*, **9**, 725 (2014)
- ³⁸ M. E. Moustaqim, A. E. Kaihal, M. E. Marouani, S. Men-La-Yakhaf, M. Taibi *et al.*, *Sustain. Chem. Pharm.*, **9**, 63 (2018), <https://doi.org/10.1016/j.scp.2018.06.002>
- ³⁹ C. Heitner, D. R. Dimmel and J. A. Schmidt, in “Lignin and Lignans: Advances in Chemistry”, edited by C. Heitner, Boca Raton, CRC Press, 2010
- ⁴⁰ A. Tejado, C. Peña, J. Labidi, J. M. Echeverria and I. Mondragon, *Bioresour. Technol.*, **98**, 1655 (2007), <https://doi.org/10.1016/j.biortech.2006.05.042>
- ⁴¹ S. K. Lagergren, *K. Sven. Vetensk. Akad. Handl.*, **24**, 1 (1898)
- ⁴² Y. S. Ho and G. McKay, *Process Biochem.*, **34**, 451 (1999), [https://doi.org/10.1016/S0032-9592\(98\)00112-5](https://doi.org/10.1016/S0032-9592(98)00112-5)
- ⁴³ Y. S. Ho and G. McKay, *Water Res.*, **34**, 735 (2000), [https://doi.org/10.1016/S0043-1354\(99\)00232-8](https://doi.org/10.1016/S0043-1354(99)00232-8)
- ⁴⁴ R. Bouhdadi, S. Benhadi, S. Molina, B. George, M. El Moussaouiti *et al.*, *Maderas*, **13**, 105 (2011), <https://doi.org/10.4067/S0718-221X2011000100009>
- ⁴⁵ O. Khelifi, I. Mehrez, W. Ben Salah, F. Ben Salah, M. Younsi *et al.*, *Larhyss J.*, **28**, 135 (2017)
- ⁴⁶ Q. Feng, H. Cheng, F. Chen, X. Zhou, P. Wang *et al.*, *J. Wood Chem. Technol.*, **36**, 173 (2016), <https://doi.org/10.1080/02773813.2015.1104546>
- ⁴⁷ C. Patawat, K. Silakate, S. Chuan-Udom, N. Supanchaiyamat, A. J. Hunt *et al.*, *RSC Adv.*, **10**, 21082 (2020), <https://doi.org/10.1039/D0RA03427D>
- ⁴⁸ L. Mouni, L. Belkhiri, J.-C. Bollinger, A. Bouzaza, A. Assadi *et al.*, *Appl Clay Sci.*, **153**, 38 (2018), <https://doi.org/10.1016/j.clay.2017.11.034>
- ⁴⁹ A. Kriaa, N. Hamdi and E. Srasra, *Russ. J. Phys. Chem.*, **85**, 279 (2011), <https://doi.org/10.1134/S0036024411020191>
- ⁵⁰ I. Langmuir, *J. Am. Chem. Soc.*, **38**, 2221 (1916), <https://doi.org/10.1021/ja02268a002>
- ⁵¹ H. Freundlich, *J. Phys. Chem.*, **57**, 385 (1907), <https://doi.org/10.1515/zpch-1907-5723>
- ⁵² K. Mahmud, M. Azharul Islam, A. Mitsionis, T. Albanis and T. Vaimakis, *Desalin. Water Treat.*, **41**, 170 (2012), <https://doi.org/10.1080/19443994.2012.664699>
- ⁵³ M. Šljivić, I. Smičiklas, I. Plečaš and M. Mitrić, *Chem. Eng. J.*, **148**, 80 (2009), <https://doi.org/10.1016/j.cej.2008.08.003>
- ⁵⁴ C. Yang, *J. Colloid Interface Sci.*, **208**, 379 (1998), <https://doi.org/10.1006/jcis.1998.5843>
- ⁵⁵ M. Hasnain Isa, L. Siew Lang, F. A. H. Asaari, H. A. Aziz, N. Azam Ramli *et al.*, *Dyes Pigm.*, **74**, 446 (2007), <https://doi.org/10.1016/j.dyepig.2006.02.025>
- ⁵⁶ A. Albadarin, C. Mangwandi, G. Walker, S. Allen and M. Ahmad, *Chem. Eng. Trans.*, **24**, 1297 (2011), <https://doi.org/10.3303/CET1124217>
- ⁵⁷ M. Tadashi, “Application of Thermodynamics to Biological and Materials Science”, InTech, 2011
- ⁵⁸ O. S. Benturki, A. Donnot, S. Molina, A. Merlin and F. Addoun, *J. Soc. Alger. Chim.*, **18**, 7 (2008)
- ⁵⁹ F. Mashkoo and A. Nasar, *Cellulose*, **27**, 2613 (2020), <https://doi.org/10.1007/s10570-019-02918-8>
- ⁶⁰ Z. A. Ghani, M. S. Yusoff, N. Q. Zaman, M. F. M. A. Zamri and J. Andas, *Waste Manage.*, **62**, 177 (2017), <https://doi.org/10.1016/j.wasman.2017.02.026>
- ⁶¹ J. J. Salazar-Rabago, R. Leyva-Ramos, J. Rivera-Utrilla, R. Ocampo-Perez and F. J. Cerino-Cordova, *Sustain. Environ. Res.*, **27**, 32 (2017), <https://doi.org/10.1016/j.serj.2016.11.009>
- ⁶² R. Zhang, Y. Zhou, X. Gu and J. Lu, *Clean - Soil Air Water*, **43**, 96 (2015), <https://doi.org/10.1002/clen.201300818>
- ⁶³ J. Bortoluz, F. Ferrarini, L. R. Bonetto, J. da Silva Crespo and M. Giovanela, *Cellulose*, **27**, 6445 (2020), <https://doi.org/10.1007/s10570-020-03254-y>
- ⁶⁴ S. P. Mishra, A. R. Patra and S. Das, *Biointerface Res. Appl. Chem.*, **11**, 7410 (2021), <https://doi.org/10.33263/BRIAC111.74107421>